

OPTIMIZATION OF A LARGE APERTURE DIPOLE MAGNET FOR BARYONIC MATTER STUDIES AT NUCLOTRON

*P. G. Akishin, A. Yu. Isupov, A. N. Khrenov, P. K. Kurilkin,
V. P. Ladygin¹, S. M. Piyadin, N. D. Topilin*

Joint Institute for Nuclear Research, Dubna

The aperture of the SP41 dipole magnet has been enlarged for the studies of dense baryonic matter properties at Nuclotron. The homogeneity of the magnetic field in the magnet centre has been improved. The measurement results of the magnetic field components and integral are compared with the results of the 3D TOSCA calculations.

Для изучения свойств плотной барионной материи на нуклотроне была расширена апертура дипольного магнита СП41. Улучшена однородность магнитного поля в центре магнита. Результаты измерения компонент и интеграла магнитного поля сравниваются с результатами расчетов 3D TOSCA.

PACS: 07.55.Db; 29.30.Aj

INTRODUCTION

The major goal in the studies of the dense baryonic matter at Nuclotron (BM@N project) [1] is the measurement of strange and multistrange baryons and mesons in heavy-ion collisions at the beam energies between 2A and 6A GeV [2]. The physics program can be extended to the measurements of the in-medium effects for strange particles decaying in hadronic modes [3], hard probes and correlations [4], spin and polarization effects [5,6], etc.

For these purposes an experimental set-up will be installed at the 6V beamline in the fixed-target hall of Nuclotron. The 6V beamline contains the quadrupole lenses doublet, two dipole magnets allowing one to correct the beam position in the vertical and horizontal planes, and the large aperture SP41 dipole magnet for the momentum measurements [1]. The first results with the relativistic deuteron [7] and carbon [8] beams demonstrated the feasibility of the dense baryonic matter studies with light nuclei using the 6V beamline infrastructure.

The modified SP41 dipole magnet will be used as an analyzing magnet [1]. Initially, the length of the magnet pole along the beam was 2.50 m, the width in the horizontal direction was 1.70 m and the height was about 0.75 m. This magnet had also a hole for the photocamera in

¹E-mail: vladygin@jinr.ru

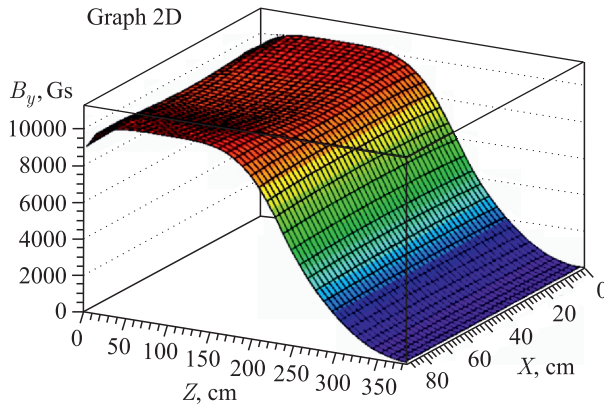


Fig. 1. The vertical component B_y of the magnetic field in the centre of the SP41 magnet before the modification

up to 1.05 m and the hole in the upper pole and horizontal beams has been filled by the steel-15. In this paper, the results of the magnetic field measurements are presented for the modified SP41 dipole magnet. These results are compared with the 3D magnetic field TOSCA calculations.

1. MAGNETIC FIELD CALCULATIONS

The magnetic field calculations for the modified SP41 dipole magnet have been performed using the 3D TOSCA code [9]. Steel-10, steel-15, and copper were taken as the material for the yoke, magnet poles, and coils, respectively. The coordinate system was chosen as follows:

X -axis is perpendicular to the beam direction in the horizontal plane, Y is vertical and Z is along the beam and parallel to the magnet poles. The 3D model of the modified SP41 dipole magnet for the magnetic field TOSCA calculations is presented in Fig. 2.

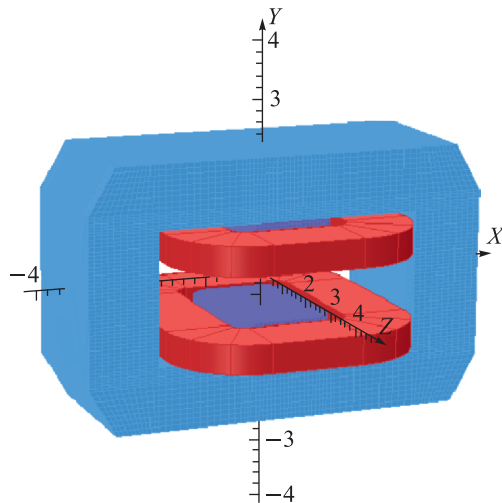


Fig. 2. The SP41 dipole magnet model for the magnetic field TOSCA [9] calculations

the upper pole since it was used previously for the experiments with streamer chamber. As a result, the magnetic field components demonstrated the nonuniform behaviour. The 2D dependence of the magnetic field vertical component B_y of the nonmodified SP41 magnet in XZ plane is shown in Fig. 1.

However, the detection of multistrange baryons requires the large aperture silicon tracking system placement into the homogeneous magnetic field [1, 2, 6]. The SP41 magnet was modified to satisfy this requirement, namely, the distance between the poles has been enlarged

The 3D TOSCA calculation results for the magnetic field vertical component B_y in the centre of the modified SP41 magnet along the beam direction are demonstrated in Fig. 3. The current in the coils was taken as 1900 A. The maximal value of the vertical component B_y was found to be ~ 0.9 T. The field integral is ~ 2.9 T·m, which is approximately 30% less than for the nonmodified SP41 magnet.

The 2D distributions in XZ plane of the magnetic field vertical component B_y of the modified SP41 magnet at $Y = 0$ cm (centre

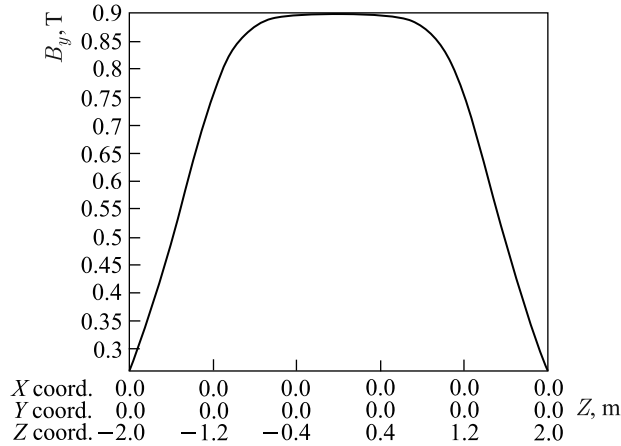


Fig. 3. The 3D TOSCA calculation results for the magnetic field vertical component B_y in the centre of the modified SP41 magnet along the beam direction

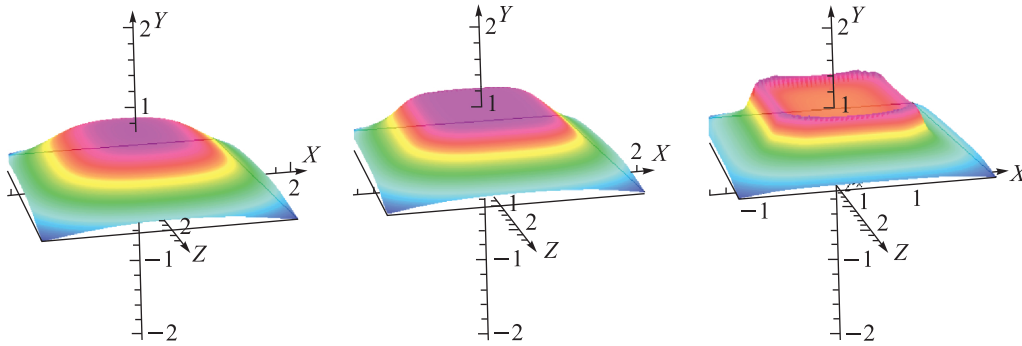


Fig. 4. From left to right: 2D distributions in XZ plane of the magnetic field vertical component B_y of the modified SP41 magnet at $Y = 0$ cm (centre of the magnet), $Y = 30$ cm, and $Y = 50$ cm

of the magnet), $Y = 30$ cm, and $Y = 50$ cm are presented in the left, middle, and right panels in Fig. 4. The field demonstrates very smooth behaviour except the region around pole of the magnet ($Y = 50$ cm). The 3D results for B_y , B_x , and B_z components of the magnetic field were incorporated into the BM@N setup description for the simulation software [6].

2. COMMISSIONING OF THE SP41 MAGNET

During 2012–2013, the warm SP41 dipole magnet has been significantly modernized. The magnet vertical gap has been enlarged by 30 cm up to 1.05 m. The upper pole and upper horizontal beams have been filled by steel-15 in order to improve the magnetic field homogeneity. The upper coil (with renovated pole and horizontal beams) and lower coil alone have been rotated by 180° in the horizontal plane to provide optimal access to the magnet infrastructure and detectors inside the BM@N experimental zone [1]. The magnet



Fig. 5. The view of modernized SP41 dipole magnet

infrastructure, namely, pipes for cooling water, the current leads, and diagnostics, have been also rotated by 180° and renovated. The view of modernized SP41 dipole magnet is presented in Fig. 5.

The commissioning of the SP41 magnet has been performed in two steps. Firstly, the operation of the magnet with the 1650 A current in the coils has been checked several times during several hours. Second step includes the measurements of the magnetic field in the centre of the magnet, the magnetic field integral, and magnetic fringe field within working range of the current in the coils (up to 1960 A).

The measurements of the vertical component B_y of the magnetic field in the centre of modernized SP41 dipole magnet ($X = 0$, $Y = 0$, $Z = 0$) have been performed using the planar Hall probe [10]. The B_y in the centre of modernized SP41 dipole magnet as a function of the current in the coils is shown in Fig. 6. The dashed curve is the result of the quadratic function approximation. The B_y demonstrates the linear dependence on the current with

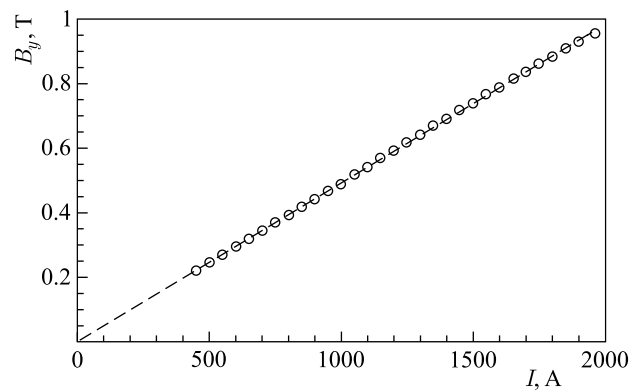


Fig. 6. The vertical component B_y of the magnetic field in the centre of modernized SP41 dipole magnet as a function of the current in the coils [10]. The dashed curve is the result of the quadratic function approximation

negligible contribution of the quadratic term. The B_y at 1900 A is equal to (0.933 ± 0.003) T being in good agreement with the 3D TOSCA calculations shown in Fig. 2.

The measurements of the magnetic field integral $\int B dl$ of modernized SP41 dipole magnet have been performed using the method of the current-carrying filament [10]. The magnetic field integral $\int B dl$ of modernized SP41 dipole magnet as a function of the current in the coils is shown in Fig. 7. The dashed curve is the result of the quadratic function approximation. The magnetic field integral $\int B dl$ is equal to (2.986 ± 0.009) T · m at 1900 A. The nonlinear contribution is about 5%. The measured value is in good agreement with the 3D TOSCA calculation results [1]. The field integral provides the bending angle of ~ 70 mrad for charged particles with $p/Z = 13$ GeV/c. On the other hand, since the saturation effect for the magnetic field integral is not observed at 1900 A, the current value in the coils can be increased. This will provide larger bending angle and better momentum resolution.

The measurements of the magnetic field $|B|$ at $X = 0.2$ m, $Y = -0.22$ m, $Z = 1.6$ m have been performed using the planar 3D Hall probe described in detail in [1]. The position of this

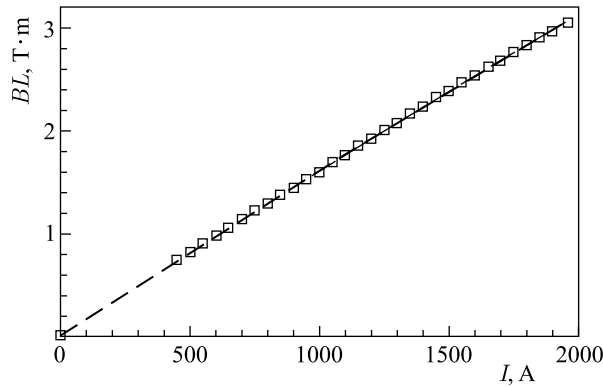


Fig. 7. The magnetic field integral $\int B dl$ of modernized SP41 dipole magnet as a function of the current in the coils [10]. The dashed curve is the result of the quadratic function approximation

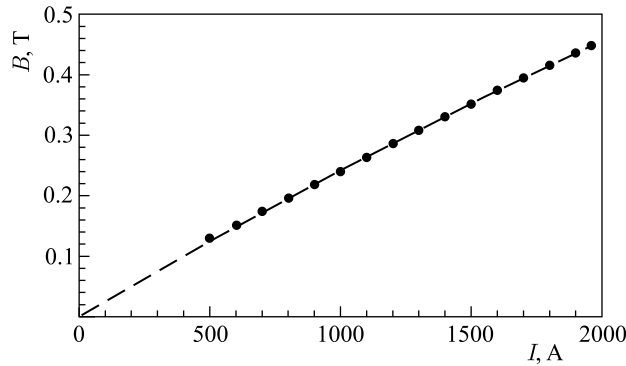


Fig. 8. The magnetic field $|B|$ measured with the planar 3D Hall probe [1] at $X = 0.2$ m, $Y = -0.22$ m, $Z = 1.6$ m as a function of the current in the coils. The dashed curve is the result of the quadratic function approximation

point is out of the magnet poles. The measured magnetic field $|B|$ as a function of the current value in the coils is shown in Fig. 8. The dashed curve is the result of the quadratic function approximation. The $|B|$ demonstrates the non-negligible contribution of the quadratic term at large values of the current in the coils. For instance, the nonlinear contribution is about 12% at the current value of 1900 A. Therefore, the fringe field demonstrates the saturation effect at large currents in the coils, which is absent for the field in central region of the magnet.

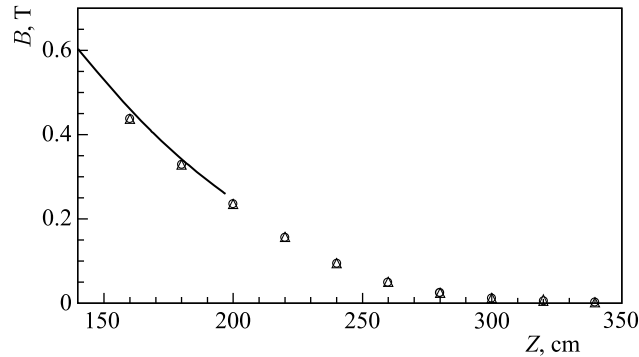


Fig. 9. The magnetic field $|B|$ for the current value in the coils of 1900 A as a function of Z coordinate ($X = 0.2$ m and $Y = -0.22$ m). The circles and triangles are the data obtained with the planar and coaxial 3D Hall probes [1], respectively. The solid curve is the result of the 3D TOSCA calculation scaled by factor 0.92

The measurements of the fringe magnetic field as a function of the distance from the magnet centre Z at fixed values of $X = 0.2$ m and $Y = -0.22$ m coordinates have been performed using the planar and coaxial 3D Hall probes [1]. The magnetic field $|B|$ for the current value in the coils of 1900 A as a function of Z coordinate is shown in Fig. 9. The circles and triangles represent the data obtained with the planar and coaxial 3D Hall probes [1], respectively. One can see that the results obtained by these two probes are in good agreement. The solid curve is the result of the 3D TOSCA calculation scaled by factor 0.92. The shape of the measured magnetic field $|B|$ reproduces the TOSCA results. The observed difference can be recovered by the optimization of the SP41 dipole magnet model for the magnetic field TOSCA [9] calculations.

CONCLUSIONS

- The SP41 dipole magnet has been modernized for the studies of dense baryonic matter properties at Nuclotron. Namely, the magnet vertical gap has been enlarged up to 1.05 m to increase the angular acceptance for detection of hyperons [2, 5, 6], the magnetic field homogeneity improvement by the filling of the existed hole in the upper pole and horizontal beams by steel-15 has been achieved, the renovation of the magnet infrastructure has been made.
- The magnetic field in the centre of the magnet and out of the poles as well as the field integral have been measured as a function of the current value in the coils. The value of the magnetic field in the magnet centre and the field integral at 1900 A are in good agreement

with the results of the 3D TOSCA calculations, while the measured fringe field at the same current is several percents below the calculated one.

- Further steps are the measurements of the magnetic field components along the optical axis of the SP41 magnet and 3D mapping of the magnetic field.

Acknowledgements. The authors thank the technical services of LHEP participated in the modification of the SP41 dipole magnet, especially, G. S. Berezin, I. Ya. Nefediev, A. V. Shabunov, V. I. Sharapov. The authors are grateful to P. A. Rukoyatkin for the magnetic measurements, I. A. Bolshakova and S. Timoshin for their assistance in the use of the 3D Hall probes. The work has been supported in part by RFBR under grant No. 13-02-00101a.

REFERENCES

1. *Ablyazimov T. O. et al. (BM@N Collab.)*. Conceptual Design Report of BM@N. <http://nica.jinr.ru/files/BM@N/BMN-CDR.pdf>.
2. *Ladygin V. P. et al. (BM@N Collab.)*. Study of Strange Matter Production in the Heavy-Ion Collisions at Nuclotron // Proc. of Baldin Seminar ISHEPP-XXI. 2012. P. 038.
3. *Bratkovskaya E. et al.* In-Medium Effects on Strangeness Production // Nucl. Phys. A. 2013. V. 914. P. 387.
4. *Vasiliev T. A., Ladygin V. P., Malakhov A. I.* Energy Dependence of the High p_T Pion Production and C_2 Azimuthal Correlation in Heavy-Ion Collisions in the Experiments with Fixed Target // Nucl. Phys. Proc. Suppl. B. 2011. V. 219–220. P. 312.
5. *Ladygin V. P., Jerusalemov A. P., Ladygina N. B.* Polarization of Λ^0 Hyperons in Nucleus–Nucleus Collisions at High Energies // Phys. Part. Nucl. Lett. 2010. V. 7. P. 349.
6. *Ladygin V. P. et al.* Experimental Program for Baryonic Matter Studies // Proc. of the XV Advanced Research Workshop on High Energy Spin Physics (DSPIN-13), Dubna, Oct. 8–12, 2013 / Ed. by A. V. Efremov and S. V. Goloskokov. Dubna: JINR, 2014. P. 239.
7. *Terekhin A. A. et al.* Preparation of Experiments to Study Light Nuclei Structure at Nuclotron // Proc. of Baldin Seminar ISHEPP-XXI. 2012. P. 005.
8. *Piyadin S. M. et al.* First Extraction of the 3.42A GeV ^{12}C Beam for Studies of Baryonic Matter at Nuclotron // Phys. Part. Nucl. Lett. 2012. V. 9. P. 589.
9. OPERA-3d User Guide. <http://www.lepp.cornell.edu/critten/opera/user-3d.pdf>.
10. *Rukoyatkin P. A.* Private Communication.

Received on September 10, 2014.